Determination of Green's Function Matrix for Multiconductor and Anisotropic Multidielectric Planar Transmission Lines: A Variational Approach

FRANCISCO MEDINA AND MANUEL HORNO, MEMBER, IEEE

Abstract—**In this paper, a set of simple recurrence formulas to evaluate the Green's function matrix for a generic multiconductor and multidielectric planar transmission system with arbitrary rectangular boundary conditions is obtained. Combining these formulas with the variational technique in the spectral domain, two useful algorithms to calculate the capacitance matrix of a very wide range of practical configurations are proposed. Upper and lower bounds on mode capacitances are obtained by using both algorithms. A number of practical structures have been analyzed and their most interesting features discussed. The method is very versatile and can handle a large class of MIC configurations, no matter how complex the planar structure.**

I. Introduction

As IS WELL KNOWN, the quasi-TEM approximation is reasonable in many cases if the cross-sectional dimensions of inhomogeneous transmission lines are much smaller than the wavelength to be used. Therefore, the calculation of the characteristic mode capacitances of planar transmission lines is useful for the design of MIC structures. The study of propagation parameters of such structures has been achieved by using several methods, such as mapping theory [1] and finite differences [2]. One of them, involving variational techniques in the spectral domain, has been successfully applied to solve a great number of planar configurations [3]–[12]. This is a very efficient numerical technique easily applicable to many microstrip line configurations. This method requires the analytical determination of the Green's function of the structure in question in the spectral domain. Usually the conductor strips are located at only one of the dielectric interfaces. However, the design flexibility has been increased introducing additional conductors on interfaces different from the one on which the original strips are situated [11]. A modification of the spectral-domain technique which can handle this kind of structure was reported by Itoh *et al.* [11], [12] introducing a Green's function matrix in the spectral domain for characterizing the configuration.

The Green's function is generally calculated for each particular configuration. However, when multilayered configurations are considered, this task becomes very tedious. This problem has been considered by a few authors [13]–[16]. Recently, the authors have studied this problem for open structures [17], and shielded structures with strips at only one interface [18]. In this paper, we show a new simple recurrence formula to obtain the Green's function matrix for a generic rectangular multilayered anisotropic structure having arbitrary boundary conditions at the side and at the upper and lower walls, and several strips located on more than one interface (see Fig. 1). Therefore, the formulation in this paper is quite general and requires no structural symmetry. Nevertheless, the symmetry can be taken into account to exploit its advantages (so that even and odd modes can be considered). The study of this generic configuration provides a method to calculate the quasi-TEM parameters of a very wide range of practical lines including lines with conductors in several interfaces.

To illustrate the power of the method, several examples of structures with conductors at only one interface and at several interfaces are included. The computation of the mode capacitances of these structures has been achieved using two stationary expressions which provide upper and lower bounds on their exact values [4]–[6]. Very accurate results have been obtained by using appropriate trial functions to approximate the surface charge density on the conductors (lower bounds) or the potential function at the interfaces where these are situated (upper bounds). In this work, a unified variational formulation for determining the line capacitances of arbitrary planar structures is shown. The number of iso/anisotropic dielectric layers and the distribution of the conductor strips are no longer obstacles for the analysis.

II. Statement of the Problem

Consider a system of planar multiconductor transmission lines in a multilayered dielectric region as shown in Fig. 1. The system is uniform in the direction perpendicu-

Manuscript received February 7, 1985; revised May 28, 1985. This work was supported in part by the "Comisión Asesora de Investigación Científica y Técnica," Spain.

The authors are with the Departamento de Electricidad y Electrónica, Facultad de Física, Universidad de Sevilla, Avda. Reina Mercedes, s/n. 41012 Seville, Spain.

0018-9480/85/1000-0933$01.00 ©1985 IEEE

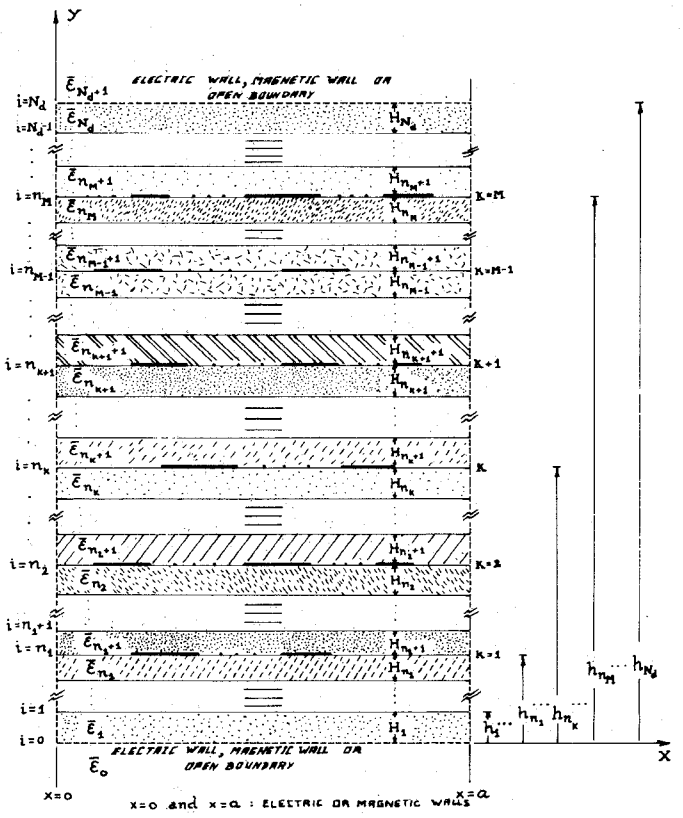

Fig. 1 Cross section of a generic multiconductor and multidielectric planar transmission system with rectangular boundary conditions.

lar to the $x-y$ plane. An arbitrary number of perfectly conducting strips are embedded in an arbitrary number N_d of dielectric layers. With the object of simplifying the computation of the capacitances per unit length, the strips will be assumed negligibly thin. The upper and lower limits of the rectangular configuration can be considered to be ground plates, magnetic walls, or open boundaries (that is, interfaces with a dielectric region extending to $y=\pm\infty$). The sidewalls ($x=0$ and $x=a$) can be electric or magnetic walls. Moreover, we will assume lossless and uniaxial anisotropic dielectric layers with no tilted optical axis: therefore, the permittivity of each layer is given by the following tensor:

$$\bar{\epsilon}_i = \epsilon_0 \begin{bmatrix} \epsilon_{xx}^{*i} & 0 \\ 0 & \epsilon_{yy}^{*i} \end{bmatrix}, \qquad i=1,\cdots,N_d. \tag{1}$$

It is evident that most useful configurations appearing in practice are particular cases of this generic system.

The objective is to determine the capacitance matrix of the multiconductor transmission-line system, or the mode capacitances if the symmetry of the structure permits us to define these modes. In this paper, we will use a variational technique in the spectral domain to achieve the corresponding calculations. The application of this method requires the knowledge of the spectral Green's function matrix for the problem structure. The derivation of a set of very simple recurrence formulas for the elements of the Green's matrix is performed in the following section.

III. Analysis—The Green's Functions Matrix

If we assume the quasi-TEM approximation to be valid, our problem reduces to solving the Laplace's equation in the $x-y$ plane subject to the appropriate boundary conditions. Instead of working in the $x-y$ plane, we will work in the discrete Fourier domain because significant advantage is gained: Green's function convolution integrals are converted into algebraic products. The boundary conditions at the vertical sidewalls ($x=0$ and $x=a$) are satisfied via the adequate definition of the discrete Fourier transform (DFT) [18]. In the spectral domain, Laplace's equation is written as follows:

$$\left\{ \frac{d^2}{dy^2} - k_n^2 \left(\frac{\epsilon_{xx}^{*i}}{\epsilon_{yy}^{*i}} \right) \right\} \tilde{\phi}_i(n,y) = 0, \qquad i=1,\cdots,N_d \tag{2}$$

where k_n is the Fourier variable and $\tilde{\phi}_i(n,y)$ is the DFT of the potential in the ith layer. The solution of (2) can be written in the following way:

$$\tilde{\phi}_i(n,y) = \frac{1}{\tilde{A}_i(n)} \left\{ \tilde{\phi}_i(n,h_i)\cdot\sinh\left[\gamma_n^i(y-h_{i-1})\right] - \tilde{\phi}_i(n,h_{i-1})\cdot\sinh\left[\gamma_n^i(y-h_i)\right] \right\}, \qquad i=1,\cdots,N_d \tag{3}$$

where

$$h_i = \sum_{k=1}^{i} H_k \qquad (H_k = \text{thickness of } k\text{th dielectric layer}) \tag{4a}$$

$$\gamma_n^i = k_n \left(\epsilon_{xx}^{*i}/\epsilon_{yy}^{*i} \right)^{1/2} \tag{4b}$$

$$\tilde{A}_i(n) = \sinh\left[\gamma_n^i H_i\right], \qquad i=1,\cdots,N. \tag{4c}$$

Applying the boundary conditions at the interfaces and letting $\tilde{\sigma}_i(n)$ be the DFT of the surface charge density on the ith interface, we can obtain the following relation:

$$\tilde{\sigma}_i(n) = \tilde{g}_{i,i-1}(n)\cdot\tilde{\phi}_i(n,h_{i-1}) + \tilde{g}_{i,i}(n)\cdot\tilde{\phi}_i(n,h_i) + \tilde{g}_{i,i+1}(n)\cdot\tilde{\phi}_{i+1}(n,h_{i+1}), \qquad i=1,\cdots,N_d \tag{5}$$

where

$$\tilde{g}_{i+1,i}(n) = \tilde{g}_{i,i+1}(n) = -\epsilon_0\cdot k_n\cdot\epsilon_{eq}^{i+1}\cdot\left[\sinh\left(k_n H_{eq}^{i+1}\right)\right]^{-1} \tag{6a}$$

$$\tilde{g}_{i,i}(n) = \epsilon_0\cdot k_n\cdot\left\{ \epsilon_{eq}^{i+1}\cdot\coth\left(k_n\cdot H_{eq}^{i+1}\right) + \epsilon_{eq}^{i}\cdot\coth\left(k_n\cdot H_{eq}^{i}\right) \right\} \tag{6b}$$

where the equivalent heights and permittivities [4]–[6], [18] are defined as follows:

$$H_{eq}^i = H_i\left(\epsilon_{xx}^{*i}/\epsilon_{yy}^{*i}\right)^{1/2} \tag{7a}$$

$$\epsilon_{eq}^i = \left(\epsilon_{xx}^{*i}\cdot\epsilon_{yy}^{*i}\right)^{1/2}. \tag{7b}$$

Now, we will consider M interfaces with conductor strips. We let $\tilde{V}_k(n)$ ($k=1,\cdots,M$) be the DFT of the potential function at these interfaces, and $\tilde{\rho}_k(n)$ ($k=1,\cdots,M$) be the DFT of the corresponding surface charge density. These quantities are related through the Green's

function matrix in the following way:

$$\tilde{V}_k(n) = \sum_{l=1}^{M} \tilde{G}_{kl}(n)\cdot\tilde{\rho}_l(n), \qquad k,l=1,\cdots,M \quad (8)$$

where M is the number of interfaces with conductor strips. Equivalently

$$\tilde{\rho}_k(n) = \sum_{l=1}^{M} \tilde{L}_{kl}(n)\cdot\tilde{V}_l(n), \qquad k,l=1,\cdots,M \quad (9)$$

where the matrices $[\tilde{G}_{kl}]$ and $[\tilde{L}_{kl}]$ are obviously related in the following way:

$$[\tilde{L}_{kl}(n)] = [\tilde{G}_{kl}(n)]^{-1}. \quad (10)$$

The elements of the $[\tilde{L}_{kl}]$ matrix can be easily obtained from (5). Noting that $\tilde{\sigma}_i(n) = \tilde{\rho}_i(n)$ at the interfaces having conductor strips and $\tilde{\sigma}_i(n) = 0$ at the rest of the interfaces, it is not difficult to realize that only the diagonal elements ($\tilde{L}_{kk}$) and the ones beside them ($\tilde{L}_{k,k+1}$ and $\tilde{L}_{k,k-1}$) are nonzero ones. We can then write

$$\tilde{\rho}_k(n) = L_{k,k-1}(n)\cdot V_{k-1}(n) + \tilde{L}_{k,k}(n)\cdot\tilde{V}_k(n) + \tilde{L}_{k,k+1}(n)\cdot V_{k+1}(n), \qquad k=1,\cdots,M. \quad (11)$$

Moreover, the symmetry of the matrix $[\tilde{G}_{k,l}(n)]$ [17] implies the symmetry of $[\tilde{\mathscr{L}}_{k,l}(n)]$. It is then evident that it is only necessary to evaluate the $\tilde{L}_{k,k}$ $(k=1,\cdots,M)$ and $\tilde{L}_{k,k-1}$ $(k=2,\cdots,M)$ elements, resulting in reduction of computation time.

Lastly, a simple algebraic manipulation of (5) permits us to find the following recurrence expressions for the elements of the $[\tilde{L}_{kl}]$ matrix: calling n_k the number of dielectric layers underneath the kth interface with conductor strips and that $n'_k = n_k - n_{k-1}$, $n''_k = n_{k+1} - n_k$, $p = n_{k-1}$, $q = n_{k+1}$, the elements of $[\tilde{L}_{kl}]$ can be expressed in the following way:

$$\tilde{L}_{k,k} = \tilde{A}_k^{n'_k} + \tilde{B}_k^{n''_k} - \tilde{g}_{n_k,n_k}, \qquad k=1,\cdots,M \quad (12)$$

$$\tilde{L}_{k,k-1} = \tilde{C}_k^{n'_k}, \qquad k=2,\cdots,M \quad (13)$$

where $\tilde{A}_k^{n'_k}$, $\tilde{B}_k^{n''_k}$, and $\tilde{C}_k^{n'_k}$ are defined by the following recurrence expressions:

$$\tilde{A}_k^1 = \tilde{g}_{p+1,p+1} \quad (14a)$$

$$\tilde{C}_k^1 = \tilde{g}_{p+1,p} \quad (14b)$$

$$\tilde{B}_k^1 = \tilde{g}_{q-1,q-1} \quad (14c)$$

$$\tilde{A}_k^j = \tilde{g}_{p+j,p+j} - \frac{\tilde{g}^2_{p+j,p+j-1}}{\tilde{A}^{j-1}} \quad (15a)$$

$$\tilde{C}_k^j = -\frac{\tilde{g}_{p+j,p+j-1}\cdot\tilde{C}_k^{j-1}}{\tilde{A}_k^{j-1}} \quad (15b)$$

$$\tilde{B}_k^j = \tilde{g}_{q-j,q-j} - \frac{\tilde{g}^2_{q-j,q-j+1}}{\tilde{B}_k^{j-1}} \quad (15c)$$

where $\tilde{g}_{i,j}(n)$ are defined in (6).

Equations (12)–(15) are valid from $k=2$ to $k=M-1$. The boundary conditions at lower ($i=0$) and upper ($i=N_d$) limit walls affects to the elements of $[\tilde{L}_{kl}]$ corresponding to $k=1$ and $k=M$. However, (12), (13), (14b), and (15) are independent of these boundary conditions. In fact, the boundary condition at the lower interface ($i=0$) is taken into account through $\tilde{A}_1^1$. Likewise, the boundary condition at the upper interface ($i=N_d$) will be taken into account via $\tilde{B}_M^1$. Next, we show the corresponding expressions for $\tilde{A}_1^1$ and $\tilde{B}_M^1$ when lower and upper limit walls are either electric walls, magnetic walls, or open boundaries.

a) Lower interface ($i=0$)

electric wall:

$$\tilde{A}_1^1 = \tilde{g}_{1,1} \quad (16a)$$

magnetic wall:

$$\tilde{A}_1^1 = \tilde{g}_{1,1} - 2\cdot k_n\cdot\epsilon^1_{eq}\cdot\left[\sinh\left(2k_nH^1_{eq}\right)\right]^{-1} \quad (16b)$$

open boundary:

$$\tilde{A}_1^1 = \tilde{g}_{1,1} - k_n\cdot\frac{\left[\epsilon^1_{eq}\cdot\left(\sinh\left(k_nH^1_{eq}\right)\right)^{-1}\right]^2}{\epsilon^0_{eq} + \epsilon^1_{eq}\cdot\coth\left(k_nH^1_{eq}\right)} \quad (16c)$$

(the superscript "0" refers to the dielectric underneath the first layer).

b) Upper interface ($i=N_d$)

electric wall:

$$\tilde{B}_M^1 = \tilde{g}_{N_d-1,N_d-1} \quad (17a)$$

magnetic wall:

$$\tilde{B}_M^1 = \tilde{g}_{N_d-1,N_d-1} - 2\cdot k_n\epsilon^{N_d}_{eq}\cdot\left[\sinh\left(2k_nH^{N_d}_{eq}\right)\right]^{-1} \quad (17b)$$

open boundary:

$$\tilde{B}_M^1 = \tilde{g}_{N_d-1,N_d-1} - k_n\cdot\frac{\left[\epsilon^{N_d}_{eq}\cdot\left(\sinh\left(k_nH^{N_d}_{eq}\right)\right)^{-1}\right]^2}{\epsilon^{N_d+1}_{eq} + \epsilon^{N_d}_{eq}\cdot\coth\left(k_nH^{N_d}_{eq}\right)} \quad (17c)$$

(the superscript "N_d+1" refers to the dielectric over the N_dth layer).

This way, (12)–(17) provide a set of recurrence formulas to obtain the elements of the $[\tilde{L}_{kl}]$ matrix, which can be programmed easily in a digital computer. Finally, the Green's function matrix is obtained by inverting the $[\tilde{L}_{kl}]$ matrix. Introducing these expressions in the already existing programs, without further modifications, the characteristic parameters of arbitrarily complicated configurations can be computed by using moment method or variational techniques. In the following section, two useful variational expressions are introduced, and some practical examples will be shown later.

IV. Variational Expressions

The electrostatic energy per unit length stored in a structure as shown in Fig. 1 can be expressed, by using Parseval's theorem, in the following way:

$$U_e = \frac{1}{2a} \sum_{n=1}^{\infty} \sum_{k=1}^{M} \tilde{\rho}_k(n) \cdot \tilde{V}_k(n). \tag{18}$$

From (8), (9), and (18), we can obtain two expressions for the electrostatic energy per unit length as a function of the surface charge density on the strips or as a function of the potential at these interfaces

$$U_e = \frac{1}{2a} \sum_{n=1}^{\infty} \sum_{k=1}^{M} \sum_{l=1}^{M} \tilde{\rho}_k(n) \cdot \tilde{G}_{kl}(n) \cdot \tilde{\rho}_l(n) \tag{19a}$$

$$U_e = \frac{1}{2a} \sum_{n=1}^{\infty} \sum_{k=1}^{M} \sum_{l=1}^{M} \tilde{V}_k(n) \cdot \tilde{L}_{kl}(n) \cdot \tilde{V}_l(n). \tag{19b}$$

If we determine the unknowns $\tilde{\rho}_k(n)$ or $\tilde{V}_k(n)$, the energy can be evaluated exactly. This is not possible in general cases, but the stationary nature of (19a) and (19b) allows us to get very accurate results by applying the Rayleigh–Ritz's optimization procedure [11], [12] and choosing a proper set of trial functions to approximate $\rho_k(x)$ or $V_k(x)$. On the other hand, (19a) and (19b) permit us to obtain upper and lower bounds on true values of the mode capacitances for a wide variety of practical structures. For instance, consider the coupled strips with tuning septums studied by Itoh *et al.* [11]. As is well known, the symmetry of this structure permits us to define two modes of propagation: an even mode and an odd mode. From (19), we can write two variational expressions for the even- and odd-mode capacitances in the following way:

$$\frac{1}{C_{e,o}} = \frac{U_e}{Q^2} = \frac{1}{2aQ^2} \sum_{n=1}^{\infty} \sum_{k=1}^{2} \sum_{l=1}^{2} \tilde{\rho}_k^{e,o}(n) \cdot \tilde{G}_{kl}(n) \cdot \tilde{\rho}_l^{e,o}(n) \tag{20a}$$

$$C_{e,o} = \frac{U_e}{V^2} = \frac{1}{2aV^2} \sum_{n=1}^{\infty} \sum_{k=1}^{2} \sum_{l=1}^{2} \tilde{V}_k^{e,o}(n) \cdot \tilde{L}_{kl}(n) \cdot \tilde{V}_l^{e,o}(n) \tag{20b}$$

where Q (charge on the strips) and V (potential of the strips) are usually considered equal to unity. Both variational expressions provide upper bounds on their exact values when trial functions for $\rho_k^{e,o}$ and $V_k^{e,o}$ are used. So, (20a) leads to lower bounds on the true value of $C_{e,o}$ and (20b) leads to upper bounds on it. This way, through an appropriate choice of trial functions, we can obtain accurate results and their margin of error. All these considerations have been taken into account to write computer programs to analyze a great number of structures. These programs were rigorously checked comparing our results for simple configurations with those obtained by conformal mapping. Some practical examples will be shown in the next section.

TABLE I
Capacitance Matrix of Asymmetric Coupled Strips on Sapphire Substrate and in Vacuum (a) Open Structure and (b) Covered Structure

(a)

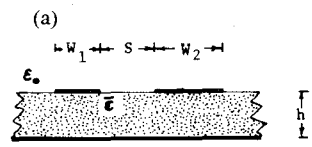

$W_2/h = 1.$
$S/h = 2.$
$\varepsilon^*_{xx} = 9.4$
$\varepsilon^*_{yy} = 11.6$

W_1/h	C_{11}/ε_0	C_{22}/ε_0	C_{12}/ε_0	C^0_{11}/ε_0	C^0_{22}/ε_0	C^0_{12}/ε_0
0.50	15.869	22.179	-1.437	2.357	3.096	-0.497
1.25	25.207	22.185	-1.558	3.437	3.103	-0.579
2.00	34.136	22.185	-1.599	4.380	3.105	-0.519

(b)

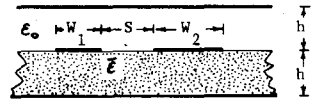

W_1/h	C_{11}/ε_0	C_{22}/ε_0	C_{12}/ε_0	C^0_{11}/ε_0	C^0_{22}/ε_0	C^0_{12}/ε_0
0.50	16.169	22.767	-1.238	2.720	3.780	-0.252
1.25	25.955	22.771	-1.295	4.289	3.781	-0.266
2.00	35.420	22.771	-1.299	5.794	3.781	-0.266

V. Numerical Results

Combining the general formulas presented in (19) or (20) with (12)–(17) proposed in this work and applying subsequently the Rayleigh–Ritz's procedure in a similar way to the one reported in [4]–[6], [11], numerical data have been generated on the quasi-static parameters of several significant structures.

Before generating these numerical results, a set of adequate basis functions was selected. Different choices of basis functions were compared, and, finally, we selected a set of functions similar to the one reported in [18], which includes the nature of the charge distribution and the potential function near the edges of the strips. The method was checked with numerical and graphic results appearing in the literature [7]–[12], and a firm agreement was found. Next, we will illustrate the theory with some practical examples.

Example 1

Let us consider the pair of asymmetrical coupled microstrips touching a sapphire dielectric slab over a conducting plane, as is shown in Fig. (a) of Table I. The capacitance matrix is easily obtained by evaluating the electrostatic energy per unit length of this configuration when: a) conductor 1 has charge Q and conductor 2 has charge zero, b) conductor 2 has charge Q and conductor 1 has charge zero, and c) both conductors have charge Q. Normalized elements of the capacitance matrix (obtained for several dimensions) C_{ij}/ϵ_0 are shown in this table for (a) open and (b) covered versions. The effects of the sidewalls are neglected when $a/h \gg 1$. The capacitance matrix in

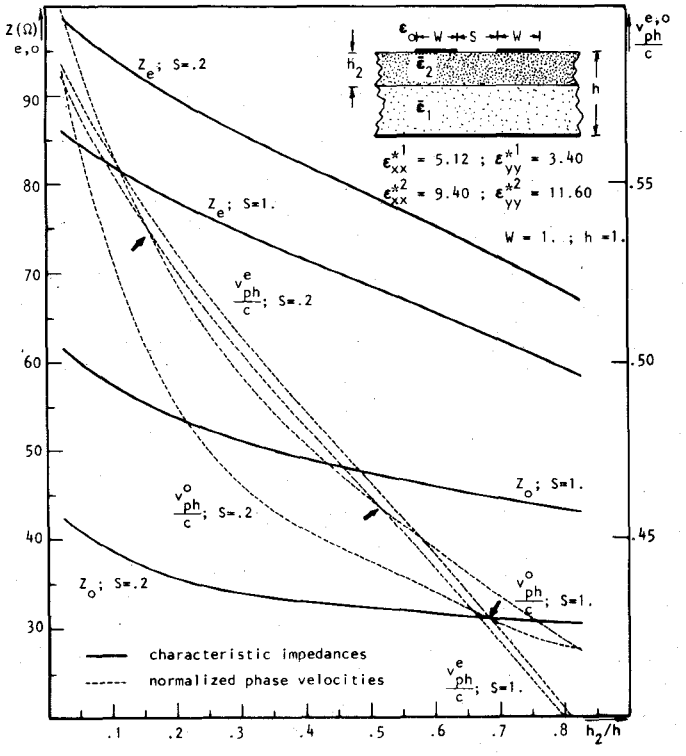

Fig. 2. Even- and odd-mode impedances and phase velocities for symmetrycal coupled strips on sapphire-boron nitride substrate. Matching points for mode phase velocities are marked with arrows.

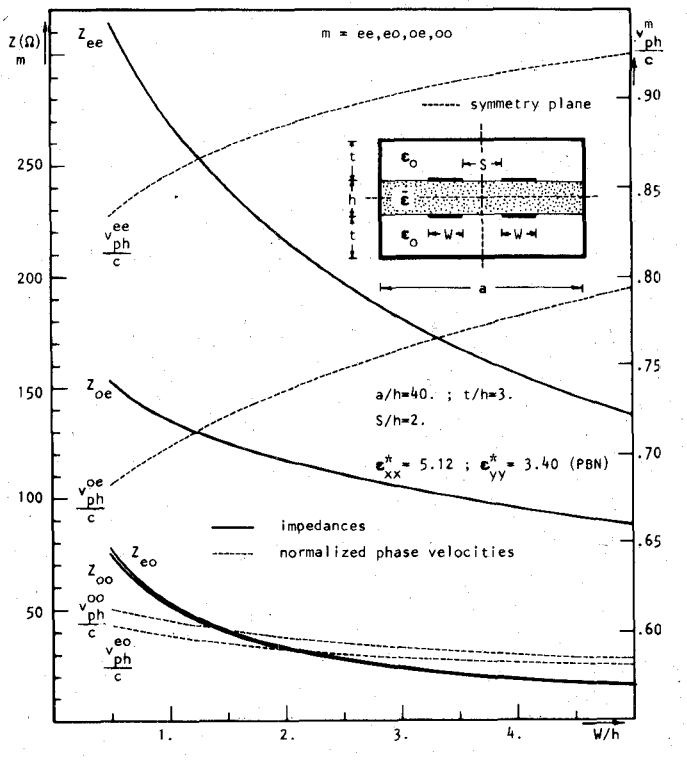

Fig. 3. Mode impedances and phase velocities versus strip width for broadside edge-coupled suspended strips on boron nitride substrate.

vacuum (C^0_{ij}), when the dielectric is removed, has also been tabulated.

Example 2

This is another example of an MIC structure having conductor strips at only one interface, but, in this case, two dielectric layers are involved (see Fig. 2): a pair of symmetrical coupled strips on a double layer sapphire-boron nitride substrate is considered. Even- and odd-mode impedances and normalized phase velocities for two values of S versus the h_2/h ratio are represented. It must be noted that even- and odd-mode phase velocities can be equalized by varying the h_2/h ratio. As is well known, this fact is important in order to improve the directivity of MIC directional couplers.

Example 3

In this case, we consider two structures with conductor strips at two different interfaces: the broadside edge-coupled suspended microstrip lines and broadside edge-coupled inverted microstrip lines (see Figs. 3 and 4, respectively). However, because of their symmetry, both structures admit four independent modes of propagation: even–even (ee), even–odd (eo), odd–even (oe), and odd–odd (oo) modes. Each of these modes can be treated as independent configurations having only one strip at only one interface by imposing the suitable boundary conditions at the symmetry planes. So, we must evaluate only the $\tilde{L}_{11}$ element of the Green's function matrix to analyze the structure in question. Propagation parameters versus strip width have been drawn in Figs. 3 and 4 for

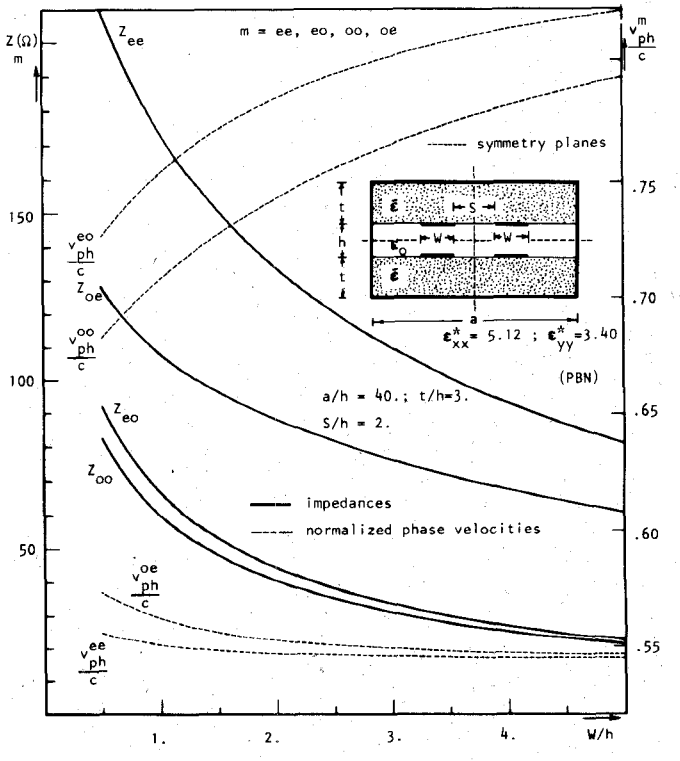

Fig. 4. Mode impedances and phase velocities versus strip width for broadside edge-coupled inverted strips on boron nitride substrate.

TABLE II
UPPER (−) AND LOWER (+) BOUNDS ON MODE IMPEDANCES FOR SINGLE AND COUPLED SUSPENDED MICROSTRIPS WITH TUNING SEPTUMS ON SAPPHIRE SUBSTRATE

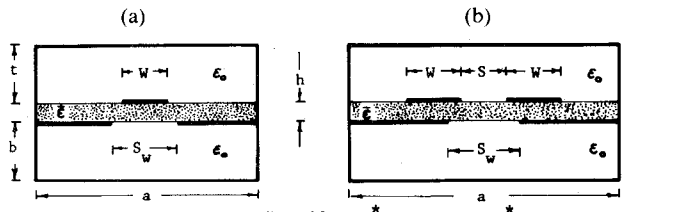

$t/h = 5.$; $b/h = 5.$; $a/h = 10.$ $\epsilon^*_{xx} = 9.4$; $\epsilon^*_{yy} = 11.6$

		SINGLE			COUPLED PAIR			
W/h	S_w/h	$Z_0(\Omega)$ +	$Z_0(\Omega)$ −	S/h	$Z_e(\Omega)$ +	$Z_e(\Omega)$ −	$Z_o(\Omega)$ +	$Z_o(\Omega)$ −
0.2	1.0	89.87	90.57	0.2	200.3	200.5	73.70	74.35
				0.6	174.7	175.3	99.74	100.3
				1.0	160.3	161.5	112.4	112.8
	4.0	135.4	136.7	0.2	288.7	290.9	74.34	74.96
				0.6	261.4	263.9	102.4	102.8
				1.0	244.4	247.1	117.8	118.1
2.0	1.0	33.40	33.42	0.2	65.23	65.27	34.99	35.02
				0.6	61.41	61.47	42.11	42.11
				1.0	58.59	58.69	45.44	45.45
	4.0	74.13	74.47	0.2	124.3	125.3	40.09	40.12
				0.6	115.5	116.3	50.55	50.57
				1.0	107.3	107.9	56.04	56.08
SAPPHIRE SUBSTRATE					EVEN MODE		ODD MODE	

+ Upper bound algorithm
− Lower bound algorithm

each of these structures considering a boron nitride substrate.

Example 4

Two interesting practical configurations having conductor strips at two interfaces are single and coupled suspended microstrip lines with tuning septums (see Figs. (a) and (b) in Table II). These configurations have been analyzed by Itoh and Hebert in [11] considering an isotropic substrate. In order to show the accuracy of the method in this paper, characteristic impedances for single and coupled configurations have been calculated by using the variational expressions for the mode capacitances given in (20a) and (20b). Results obtained with both algorithms have been tabulated in Table II. It is apparent that upper bounds on mode capacitances (+) lead to lower bounds on mode impedances and vice versa. Differences between data obtained with each algorithm are always less than 1 percent. Nevertheless, the lower bound algorithm is recommended because it spends less computation time and it provides more accurate results. On the other hand, Figs. 5 and 6 show impedances and normalized phase velocities versus slit width (S_w), respectively. It must be emphasized that even-mode parameters can be tuned by changing S_w over a wide range of values, whereas the odd-mode ones are only lightly affected. Moreover, it is clearly seen that, at certain values of the slit width, phase velocities of the even and odd mode coincide. As stated above, this phenomenon is useful for directional coupler applications.

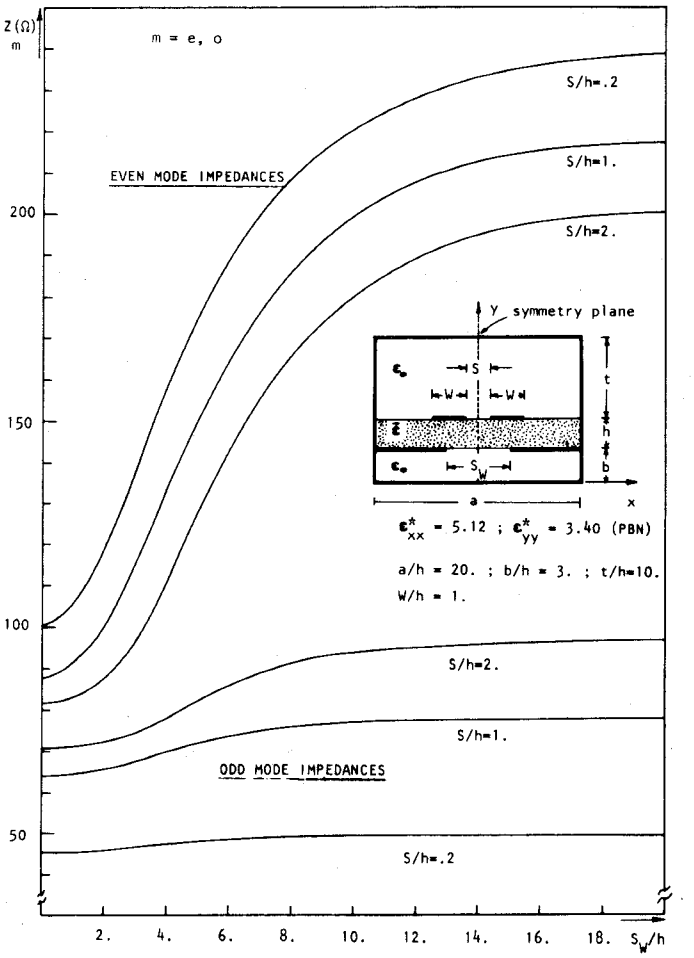

Fig. 5. Even- and odd-mode impedances for coupled suspended strips with tuning septums on boron nitride substrate versus slit width (S_w) taking the distance between the strips (S) as parameter.

Fig. 7 shows the influence of the substrate anisotropy on the characteristic parameters. Once again we can decrease the difference between even- and odd-mode phase velocities: in this case it is clear that substrates with a high $\epsilon^*_{xx}/\epsilon^*_{yy}$ ratio can improve the directivity of directional couplers designed with this configuration.

Finally, an interesting application of the method described in this paper is the study of the configurations of which the dielectric medium has a variable dielectric constant with an index gradient in the y-direction [16]. Fig. 8 illustrates the variation of the characteristic parameters for an exponential variation of the dielectric constant for a single suspended strip with tuning septums. In order to apply the theory, the dielectric thickness was subdivided into N equal intervals of constant permittivity. To obtain curves in Fig. 8, $N = 30$ was chosen: that is quite sufficient if no abrupt variation is considered. In this case, nonuniform discretization is recommended.

Before concluding this section, let us note that, although only a few simple cases have been selected to show the applications of the method, arbitrarily complicated planar configurations can be analyzed without increasing the complexity of the computer programs.

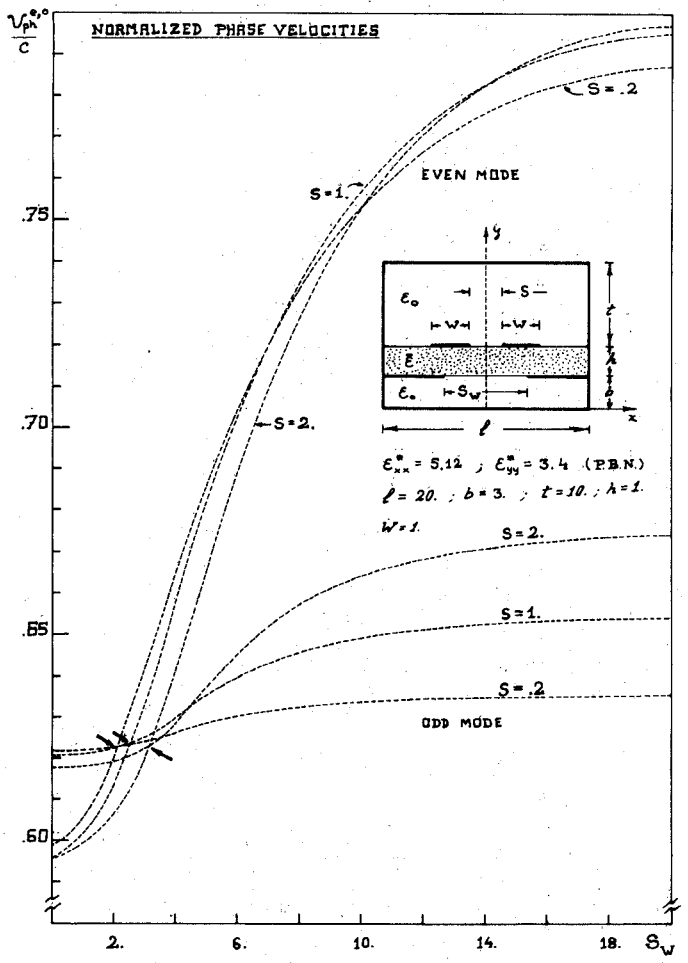

Fig. 6. Even- and odd-mode phase velocities for coupled suspended strips with tuning septums on boron nitride substrate versus slit width (S_w) taking S as parameter. Matching points for mode phase velocities are marked with arrows.

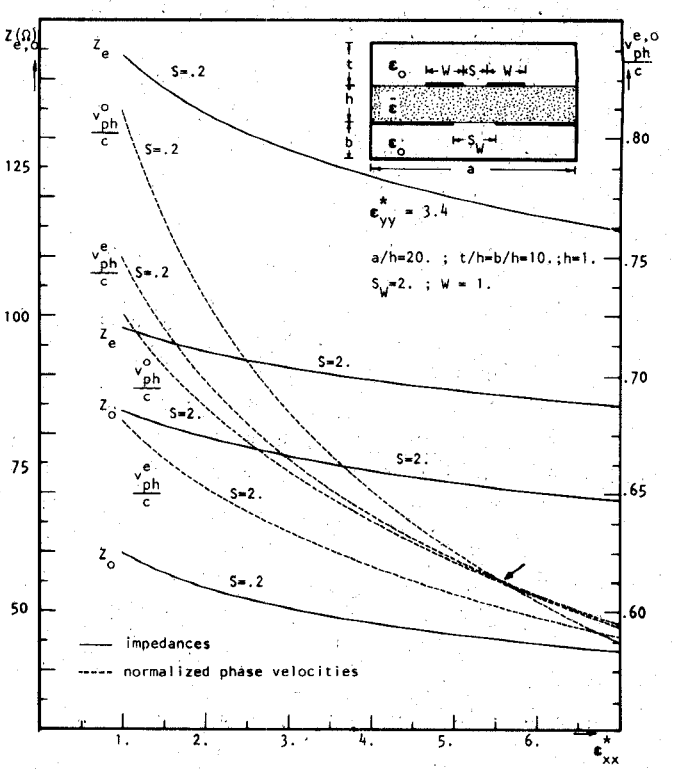

Fig. 7. Effect of the dielectric anisotropy on characteristic parameters of coupled suspended strips with tuning septums. Phase velocities of even and odd modes can be matched with highly anisotropic substrates (such as boron nitride).

By using the trial functions reported in [18], typical computation time was found to be 2–3 s (CPU time) per C_{ij} coefficient on a VAX-11/780 computer. When the number of boundaries increases, CPU time also does by approximately 0.5 s per added dielectric layer.

VI. Conclusions

In this paper, a set of simple and useful recurrence formulas to obtain the Green's function matrix associated with a multiconductor multidielectric planar transmission system with rectangular generic boundary conditions are presented. These formulas have been combined with the variational approach in the spectral domain previously used to analyze particular configurations, and, in this way, a unified formulation to solve a very wide range of microstrip-like transmission lines embedded in anisotropic substrates has been obtained. Moreover, two stationary expressions for the electrostatic energy per unit length have been proposed, each of them leading to an independent computational algorithm. In many cases, results obtained by using these algorithms are upper and lower bounds on the exact values of the mode capacitances. So, through an

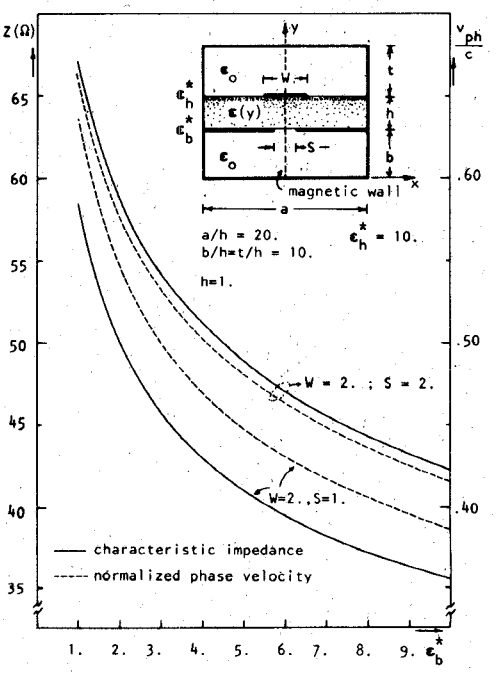

Fig. 8. Characteristic parameters of suspended microstrip with tuning septums having an exponential variation of the permittivity index of the substrate.

adequate choice of trial functions, we can get very accurate design data, and, moreover, it is possible to known the margin of error of them. This way, reliability of computed values is guaranteed.

References

[1] R. C. Callarotti and C. Gallo, "On the solution of a microstripline with two dielectrics," *IEEE Trans. Microwave Theory Tech.*, vol. MTT-32, pp. 333–339, Apr. 1984.

[2] R. P. Owens, J. E. Aitken, and T. C. Edwards, "Quasi-static characteristics of microstrip on an anisotropic sapphire substrate," *IEEE Trans. Microwave Theory Tech.*, vol. MTT-24, pp. 499–506, Aug. 1976.

[3] A. Venema, J. J. M. Dekkers, and R. F. Humphryes, "Static capacitance calculations for a surface acoustic wave interdigital transducer in multilayered media," *IEEE Trans. Microwave Theory Tech.*, vol. MTT-26, pp. 294–297, Apr. 1978.

[4] M. Horno, "Upper and lower bounds on capacitances of coupled microstrip lines with anisotropic substrates," *Proc. Inst. Elec. Eng., Microwaves, Opt. & Antennas*, vol. 129, pt. H, pp. 89–93, June 1982.

[5] ——, "Quasi-static characteristics of covered coupled microstrips on anisotropic substrates: Spectral and variational analysis," *IEEE Trans. Microwave Theory Tech.*, vol. MTT-30, pp. 1888–1892, Nov. 1982.

[6] M. Horno, F. Medina, and R. Marqués, "Quasi-static characteristic of shielded coupled microstriplines on anisotropic substrates," in *Conf. Proc. Melecon '83* (Athens), May 1983.

[7] S. K. Koul and B. Bhat, "Inverted microstrip and suspended microstrip with anisotropic substrates," *Proc. IEEE*, vol. 70, pp. 1230–1231, Oct. 1982.

[8] ——, "Propagation parameters of coupled microstrip-like transmission lines for millimeter-wave applications," *IEEE Trans. Microwaves Theory Tech.*, vol. MTT-29, pp. 1364–1370, Dec. 1981.

[9] ——, "Generalized analysis of microstrip-like transmission lines and coplanar strips with anisotropic substrates for MIC, electro-optic modulator and SAW application," *IEEE Trans. Microwave Theory Tech.*, vol. MTT-31, pp. 1051–1059, Dec. 1983.

[10] I. J. Bahl and P. Bhartia, "Characteristics of inhomogeneous broadside-coupled striplines," *IEEE Trans. Microwave Theory Tech.*, vol. MTT-28, pp. 529–535, June 1980.

[11] T. Itoh and A. S. Hebert, "A generalized spectral domain analysis for coupled suspended microstriplines with tuning septums," *IEEE Trans. Microwave Theory Tech.*, vol. MTT-26, pp. 820–826, Oct. 1978.

[12] T. Itoh, "Generalized spectral domain method for multiconductor printed lines and its application to turnable suspended microstrips," *IEEE Trans. Microwave Theory Tech.*, vol. MTT-26, pp. 983–987, Dec. 1978.

[13] Y. Chang and I. C. Chang, "Simple method for the variational analysis of a generalised N-dielectric-layer transmission line," *Electron. Lett.*, vol. 6, no. 3, pp. 49–50, Feb. 1970.

[14] Y. Chang and C.-Y. Wu, "Extension of Chang–Chang's method to analysis of generalised multilayer and multiconductor transmission-line system," *Electron. Lett.*, vol. 7, no. 2, pp. 45–47, Jan. 1971.

[15] M. Kobayashi and R. Terakado, "General form of Green's function for multilayer microstripline with rectangular side walls," *IEEE Trans. Microwave Theory Tech.*, vol. MTT-24, pp. 626–628, Sept. 1976.

[16] R. Crampagne, M. Ahmadpanah, and J. L. Guiraud, "A simple method for determining the Green's function for a large class of MIC lines having multilayered dielectric structures," *IEEE Trans. Microwave Theory Tech.*, vol. MTT-26, pp. 82–87, Feb. 1978.

[17] R. Marqués, M. Horno, and F. Medina, "A new recurrence method for determining the Green's function of planar structures with arbitrary anisotropic layers," *IEEE Trans. Microwave Theory Tech.*, vol. MTT-33, pp. 424–428, May 1985.

[18] F. Medina and M. Horno, "Upper and lower bounds on mode capacitances for a large class of anisotropic multilayered microstrip-like transmission lines," to be published in *Proc. Inst. Elec. Eng.*, pt. H.

Francisco Medina was born in Puerto Real, Spain, on November 9, 1960. He received the Licenciatura degree in physics from the University of Seville, Spain, in September 1983.

He is currently Assistant Professor of Electricity and Magnetism at the Department of Electricity and Electronics, University of Seville, where he is now studying for the Ph.D. degree. His current interests are in multiconductor planar transmission lines and MIC design.

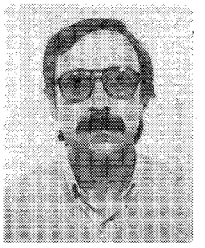

Manuel Horno (M'75) was born in Torre del Campo, Spain, on June 29, 1947. He received the degree of Licenciado in physics in June 1969, and the degree of Doctor en Ciencias in physics in January 1972, both from the University of Seville, Spain.

Since October 1969, he has been with the Department of Electricity and Electronics at the University of Seville, where he became an Assistant Professor in 1970, Associate Professor in 1975, and Titular Professor in Electricity and Magnetism. His main fields of interest include boundary-value problems in electromagnetic theory, wave propagation through anisotropic media, and microwave integrated circuits. He is presently engaged in the analysis of planar transmission lines embedded in anisotropic materials.